



The FluxEngine air-sea gas flux toolbox: simplified interface and extensions for *in situ* analyses and multiple sparingly soluble gases

Thomas Holding¹, Ian G. Ashton¹, Jamie D. Shutler¹, Peter E. Land², Philip D. Nightingale², Andrew P. Rees², Ian Brown², Jean-Francois Piolle³, Annette Kock⁴, Hermann W Bange⁴, David K. Woolf⁶, Lonke Goddijn-Murphy⁶, Ryan Pereira⁷, Frederic Paul³, Fanny Girard-Ardhuin³, Bertrand Chapron³, Gregor Rehder⁸, Fabrice Ardhuin³, Craig J. Donlon⁹

¹University of Exeter, Penryn Campus, Cornwall, TR10 9EZ, UK.

10 ²Plymouth Marine Laboratory, Prospect Place, Plymouth, PL1 3DH, UK.

³Ifremer, Univ. Brest, CNRS, IRD, Laboratoire d’Oceanographie Physique et Spatiale (LOPS), IUEM, Brest, France.

⁴GEOMAR Helmholtz Centre for Ocean Research Kiel, Marine Biogeochemistry Research Division, 24105 Kiel, Germany.

15 ⁵International Centre for Island Technology, Heriot-Watt University, Stromness, Orkney, KW16 3AW, UK.

⁶Environmental Research Institute, University of the Highlands and Islands, Thurso, KW14 7EE, UK

⁷The Lyell Centre, Heriot-Watt University, Research Avenue South, Edinburgh, EH14 4AS, UK.

⁸Leibniz-Institute for Baltic Sea Research Warnemünde, 18119 Rostock, Germany.

20 ⁹European Space Agency, Noordwijk, The Netherlands.

Correspondence to: Thomas Holding (t.m.holding@exeter.ac.uk)

25 **Abstract.** The flow (flux) of climate critical gases, such as carbon dioxide (CO₂), between the ocean and the atmosphere is a fundamental component of our climate and the biogeochemical development of the oceans. Therefore, the accurate calculation of these air-sea gas fluxes is critical if we are to monitor the health of our oceans and changes to our climate. FluxEngine is an open source software toolbox that allows users to easily perform calculations of air-sea gas fluxes from model, *in-situ* and Earth
30 observation data. The original development and verification of the toolbox was described in a previous publication and the toolbox is already being used by scientists across multiple disciplines. The toolbox has now been considerably updated to allow its use as a Python library, to enable simplified installation, verification of its installation, to enable the handling of multiple sparingly soluble gases and greatly expanded functionality for supporting *in situ* dataset analyses. This new functionality for
35 supporting *in situ* analyses includes user defined grids, time periods and projections, the ability to re-analyse *in situ* CO₂ data to a common temperature dataset and the ability to easily calculate gas fluxes using *in situ* data from drifting buoys, fixed moorings and research cruises. Here we describe these new capabilities and then demonstrate their application through illustrative case studies. The first case study demonstrates the workflow for accurately calculating CO₂ fluxes using *in situ* data from four research
40 cruises from the Surface Ocean CO₂ Atlas (SOCAT) database. The second case study shows that reanalysing an eight month time series of pCO₂ data collected from a fixed station in the Baltic Sea can remove errors equal to 35% of the net air-sea gas flux. The third case study demonstrates that



biological surfactants could suppress individual nitrous oxide sea-air gas fluxes by up to 13%. The final case study illustrates how a dissipation-based gas transfer parameterisation can be implemented and used. The updated version of the toolbox (version 3) and all documentation is now freely available.

1. Introduction

The exchange of climate relevant gases between the oceans and atmosphere including that of carbon dioxide (CO₂), nitrous oxide (N₂O) and methane (CH₄) is a major component of the climate system, and the ability of the oceans to absorb and desorb these gases varies both temporally and spatially. The need to monitor this exchange has been the driver for international data collation initiatives such as the Surface Ocean CO₂ Atlas (SOCAT, (Bakker *et al.*, 2016)) and the MarinE MethanE and NiTrous Oxide database (MEMENTO, Kock and Bange, 2015). These collaborative efforts are now routinely collecting, quality controlling and collating over a million new *in situ* data points each year. FluxEngine complements these initiatives by providing a standardised tool, which can robustly calculate air-sea gas fluxes from such *in situ* data, with the flexibility to incorporate new data sources and methodologies. The use of common tools and methods simplifies collaborations and accelerates advancements, both within and between scientific disciplines, through eliminating methodological or implementation-driven differences and the duplication of effort.

1.0 Overview of FluxEngine

FluxEngine is a flexible open source toolbox that allows users to easily exploit Earth observation and model data, in combination with *in situ* data, to calculate air-sea gas fluxes (Shutler *et al.*, 2016). The toolbox uses plain text-format configuration files allowing the user to configure the input data sources, the temporal period for the analysis, the structure of the air-sea gas flux calculation and user-defined gas transfer velocity parameterisations. Further optional features include the addition of random noise or bias to the input data. The calculation itself can be performed using fugacity, partial pressure or concentration data, using a bulk formulation or more accurate formulations that take into account vertical temperature gradients across the mass boundary layer, the very small layer at the surface over which gas exchange occurs. The latter approach allows a more accurate gas flux calculation and is described in detail by (Woolf *et al.*, 2016) and takes the generalised form of

$$F = k(\alpha_w fG_w - \alpha_s fG_A) \quad (1)$$

where F is the sea-to-air flux of a sparingly soluble gas G , k is the gas transfer velocity (cm h⁻¹), α_s and α_w are the solubilities of the gas above and below the surface water interface and fG_A and fG_w are the respective fugacities. Here we use ‘p’ and ‘f’ prefixes to refer to partial pressure and fugacity of a gas, respectively. Gas transfer velocity is driven by turbulence at ocean surface, caused by wind stress and wave breaking, amongst other processes. Because of the wide availability of high quality wind data products and the relative difficulty of directly measuring turbulence, it is commonplace to estimate k using a statistical relationship with wind speed, e.g. (Ho *et al.*, 2006; Nightingale *et al.*, 2000; Wanninkhof, 2014).



85 Concentration of the gas is determined by its solubility and fugacity (or partial pressure). Equation (1)
can therefore be rewritten as a product of the gas transfer velocity and the difference in gas
concentrations,

$$F = k(G_W - G_S) \quad (2)$$

90 where G_S and G_W are the concentration of the gas at and below the interface. The FluxEngine
configuration file allows users to choose the structure of the gas flux calculation (i.e. a bulk calculation,
or equation 1 or 2), the inputs and the gas transfer velocity (either by choosing an already implemented
published algorithm or through parameterising their own). The user can then run all calculations across
95 their chosen input data and the outputs are Climate Forecast (CF) standard netCDF 4.0 files that
contain data layers for each of the stages of the calculation, along with process indicator layers to aid
the understanding of the calculated gas fluxes (such as surface chlorophyll-a concentrations, the
climatological position of temperature fronts and error indicator layers).

100 Version 1.0 of FluxEngine was introduced and described by (Shutler, *et al.*, 2016), which included a
full description of the calculations, the flexibility of the toolbox, and the extensive verification of the
different calculations along with examples of its use. Since its original release the toolbox has
continued to be developed and extended based on feedback from the user communities and the needs of
specific scientific studies (e.g. Ashton *et al.*, 2016). These developments have considerably extended
105 the functionality of the toolbox and broadened the range of possible applications to which it can be
applied. At the time of writing the toolbox and resulting data have been used to quantify regional
method uncertainties (e.g. Wrobel and Piskozub, 2016; Wrobel, 2017), evaluate the impact of gas
transfer processes on regional and global gas exchange (e.g. Ashton *et al.*, 2016; Pereira *et al.*, 2018),
evaluate the European shelf sea CO₂ gas-fluxes and sink (Shutler *et al.*, 2016) and investigate
110 biological and physical controls of air-sea exchange (Henson *et al.*, 2018). FluxEngine has also been
used to identify shortfalls of current modelling approaches through the inclusion of FluxEngine outputs
within an international inter-comparison (Rödenbeck *et al.*, 2015) and is currently being used within
two pan-European carbon monitoring research infrastructure projects (EU RINGO and EU BONUS
INTEGRAL) which are part of the Integrated Carbon Observing System, ICOS. The toolbox has also
115 been incorporated within undergraduate and postgraduate teaching (e.g. at the University of Exeter
within geography, environmental science and marine biology degrees, and at Utrecht University for
computer science). Most recently the toolbox is being used by two European Space Agency (ESA)
projects to support preliminary studies for a new satellite concept (the Sea Surface Kinematics
Multiscale Monitoring, SKIM, satellite mission (Arduin *et al.*, 2018)) and to verify our understanding
120 of vertical temperature profiles and concentration gradients (as described by Woolf *et al.*, 2016)
through the analysis of a novel fiducial reference dataset. The results from these studies will be
reported elsewhere, but their needs have driven some of the advancements presented here.

This paper uses four case studies to illustrate key developments and extended capabilities now
125 contained within version 3.0 of the FluxEngine toolbox. Collectively the case studies illustrate user
selectable grids, support for calculating sea-to-air gas fluxes from time series data collected by fixed
monitoring stations and research cruises (and how to incorporate the flux outputs into the original
dataset to create a coherent time series), the ability to calculate nitrous oxide (N₂O) and methane (CH₄)



130 sea-to-air gas fluxes, the addition of a new forcing variable (kinetic energy dissipation rate) and the
ability to run ensembles of any of these calculations to characterise method uncertainties. The extensive
support for *in situ* data contained within version 3 of FluxEngine means that it can now be fully
exploited by three different scientific communities in isolation: *in situ*, model and Earth observation;
whilst the original capability to enable gas fluxes to be calculated from combinations of *in situ*, model
and Earth observation data is retained.

135

Section 2 describes the structural extensions and changes, including the automatic software installers
and verification tools (allowing users to verify the integrity of their installation). It explains how the
toolbox can now be used as a command line tool or as a Python library. Section 3 then presents the case
studies, while section 4 outlines the future direction and developments for the toolbox and section 5
140 gives conclusions. To aid the user the Appendices of this paper provide a list all of the toolbox utilities
(Sect. 6) and details of all data sets used (Sect. 7).

2. New capabilities

145 The following sections describe the extensions to the FluxEngine toolbox that are now contained within
version 3.

2.1. Installation, verification and use

FluxEngine has now been optimised for use on a standalone desktop or laptop computer, removing the
previous requirement for specialist computing facilities. Installation tools or instructions are now
150 provided for the following operating systems: Ubuntu/Debian based Linux
(*install_dependencies_ubuntu.sh*), Apple Mac (*install_dependencies_macos.sh*) and Windows
(instructions are within *FluxEngineV3_instructions.pdf*). Separate utilities (*verify_takahashi09.py* and
verify_socatv4_sst_salinity_gradients_N00.py) can then be used to verify that FluxEngine has been
successfully installed. These verification utilities run standard global sea-to-air CO₂ gas flux
155 calculations and net integrated fluxes using the (Takahashi *et al.*, 2009) sea-to-air CO₂ flux climatology
(for year 2000) and the Woolf *et al.*, (in-review) Surface Ocean CO₂ Atlas (SOCAT, Bakker *et al.*,
2016) derived sea-to-air CO₂ flux reference dataset (for year 2010). The results are then evaluated
against the published reference data provided by Holding *et al.*, (2018) and the installation is deemed
successful if all results are identical to the reference dataset within a precision of 5 decimal places. An
160 additional utility (*run_full_verification.py*) enables the user to perform a more detailed verification
against both of these climatologies by executing a suite of 12 different configurations and scenarios, the
justification for which are described within Woolf *et al.*, (in-review). Owing to the large volume of data
required to execute and verify all of these scenarios, the verification data are not packaged with the
standard FluxEngine download, but are all freely available and contained within Holding *et al.*, (2018).

165

FluxEngine is now implemented as a Python module available on a creative commons license via
<http://github.com/oceanflux-ghg/FluxEngine>. This means that FluxEngine and its accompanying
utilities can be used as command line tools (stand-alone tools or called from another piece of software)
or imported as a Python module and easily integrated with other software. This approach offers a larger
170 degree of flexibility than offered by version 1 of the toolbox and supports advanced exploitation. For
example, a simple Python script can be written to run a sensitivity analysis where ensembles of flux
calculations are required without any need to modify the underlying FluxEngine software.



175 To provide an indication of the execution time a benchmarking analysis was performed using an Intel
Core i5 5.7 GHz Laptop processor with 8GB RAM running MacOS El Capitan. The automatic
installation took ~3 minutes to complete and the basic verification script using the Woolf *et al.*, (in-
review) reference dataset (involving a global one year analysis of the gas fluxes for 2010, monthly
temporal resolution and $1^\circ \times 1^\circ$ spatial resolution) took approximately 6 minutes to complete. As the
flux calculation is sequential for each grid cell the execution time scales approximately linearly with
180 number of grid points and number of time steps. Hence, doubling the temporal resolution will
approximately double the execution time, whilst doubling the resolution of both spatial dimensions will
lead to a factor of four increase in execution time.

2.2. Flexible input data specification

185 Previous versions of FluxEngine required the user to make changes to the underlying software in order
to use new or differently formatted sources of input data. This required additional (and time
consuming) testing and verification after modifications were made, making FluxEngine less accessible
to those unfamiliar to Python programming. Two features have been added in version 3.0 to address
this issue: i) file pattern matching (through standard Unix glob patterns and custom date/time tokens,
190 described fully in *FluxEngineV3_instructions.pdf*) allows input file name format and directory structure
to be customised using the plain text configuration file, ii) optional pre-processing functions can be
used to manipulate input data after the data have been read into memory. These features can be
specified for each input variable in the configuration file and FluxEngine contains a selection of
common pre-processing functions, such as unit conversions or matrix transformation of the input data.
195 Additional custom pre-processing functions can be added and tested easily by the user without the need
to modify the core FluxEngine software, through copying and then completing the Python template
function provided within the source code (*data_preprocessing.py*). Storing the completed function into
the *data_preprocessing.py* file will then result in the custom pre-processing function being
automatically available for use in any configuration files.

200 These features make it possible to use any observational netCDF dataset by specifying the file path
and, if required, appropriate pre-processing functions. For example a custom pre-processing function
could resample the input files, followed by a transformation to change the projection. This flexibility is
conceptualised by the diagram in Fig. 1.

205

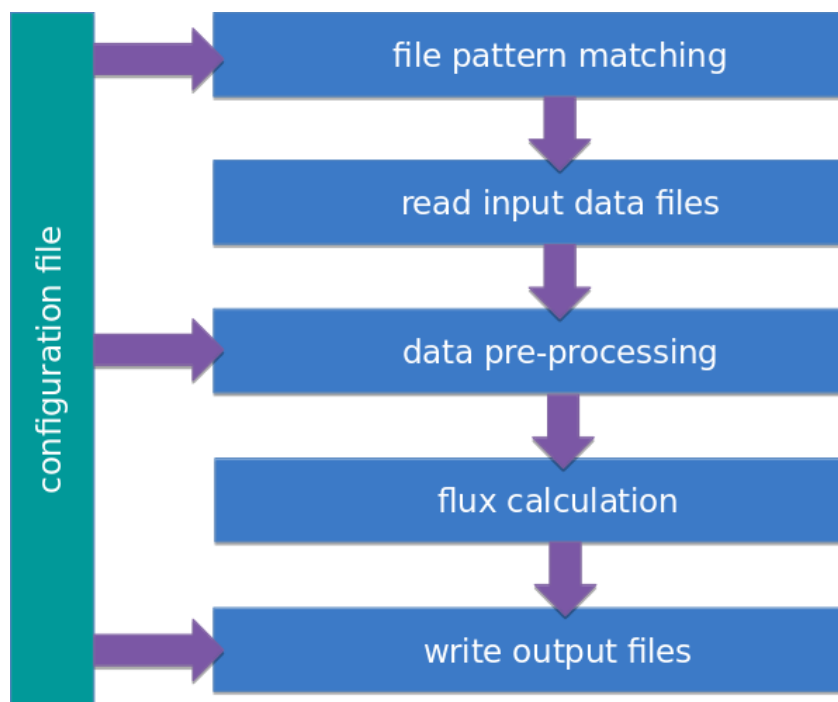


Figure 1: Conceptual diagram showing the way that input data are imported and used by FluxEngine. Single or groups of files are specified using a plain text configuration file. File names are interpreted using a subset of regular expression matching syntax (Unix glob patterns) and additional tokens are used to substitute time and date. The data pre-processing steps occur after input files are read into memory. Pre-processing functions are specified in the configuration file. Finally, the netCDF output files follow a user-specified filename and directory structure (as specified in the configuration file).

2.3. Extensive support for *in situ* data analyses

Version 1 of FluxEngine required that all input data be supplied as monthly $1^\circ \times 1^\circ$ global grids. These
210 constraints precluded its application to regional analyses and *in situ* analyses, where sub-daily or sub-
km resolutions are often more appropriate. The spatial resolution and extent can now be fully specified
by the user and regional masks can be used in conjunction with the `ofluxghg_flux_budgets.py` tool to
calculate regional net integrated fluxes. In addition, flexible start and stop times and user-specified
215 temporal resolution allows gas fluxes to be calculated for specific time intervals, e.g. the calculation
can be configured to match the temporal resolution of the *in situ* data. Furthermore, a new
configuration option allows output from multiple time points to be grouped into a single netCDF file
(rather than multiple files, one for each time point). This feature is designed to enable the calculation of
gas fluxes from fixed research stations and other scenarios in which it is more convenient to provide
220 results as a single time-series.

Improvements have been made to the bundled file conversion utilities, which convert between plain
text data formats and the netCDF format used by FluxEngine. By default, these tools use the SOCAT
format (Bakker *et al.*, 2016) for convenience, but now offer a high degree of flexibility to reflect the
variety of data formats and conventions used for storing *in situ* data. This means that the tools can be



225 used with virtually any text formatted *in situ* data files, avoiding the need for the user to convert their
data to a fixed format with predefined column names.

The new utility, *append2insitu.py*, is designed specifically for use with *in situ* data and appends
FluxEngine output as new columns within the original *in situ* data (achieved by matching spatial and
230 temporal coordinates). For example, this means that users can use SOCAT (or custom) formatted *in
situ* data as input to FluxEngine and then the results can be placed into a copy of the original input file,
allowing the user to study the calculated fluxes, gas transfer rates, gas concentrations etc. alongside
(and aligned with) their original *in situ* data. This functionality is demonstrated in case studies one and
three within this paper.

235 *In situ* fCO₂ measurements are often made using water sampled from differing depths and/or a range of
different instrument setups. A second new utility, *reanalyse_socat_driver.py* enables fCO₂
measurements to be re-analysed to a consistent temperature field at a consistent depth. This reanalysis
tool is CO₂ specific and is required for an accurate gas flux calculation as it allows the *in situ* gas
240 concentration to then be calculated at the bottom or top of the mass boundary layer, rather than
assuming that the gas concentration at some depth is representative of that at the sea surface (Woolf *et
al.*, 2016). This reanalysis is especially important if the *in situ* data consist of a collated dataset
originating from multiple instruments, sampling strategies or sources. In this situation the *in situ*
measurements are more likely to be collected from a range of different depths. It is worth noting that
245 ship draught, and thus underway measurement intake depth, can even vary on a single vessel due to
changes in sea state, ballasting or cargo. A more detailed justification of the method and a full
description of the approach are described in Goddijn-Murphy *et al.*, (2015). Whilst the reanalysis
method and utility is CO₂ specific, its applicability to alternative gases (including unreactive N₂O and
CH₄) is discussed and shown in Table 1 of (Woolf *et al.*, 2016). The impact of not performing this
250 reanalysis on a relatively large time series of CO₂ measurements through the north and south Atlantic is
demonstrated within case study one.

A typical workflow for calculating sea-to-air gas fluxes from *in situ* data using FluxEngine, and the
tools used at each step, is illustrated in Fig. 2. All of the *in situ* analysis utilities, including the use of
255 the *reanalyse_socat_driver.py* tool, are demonstrated in case studies one to three (Sect. 3).

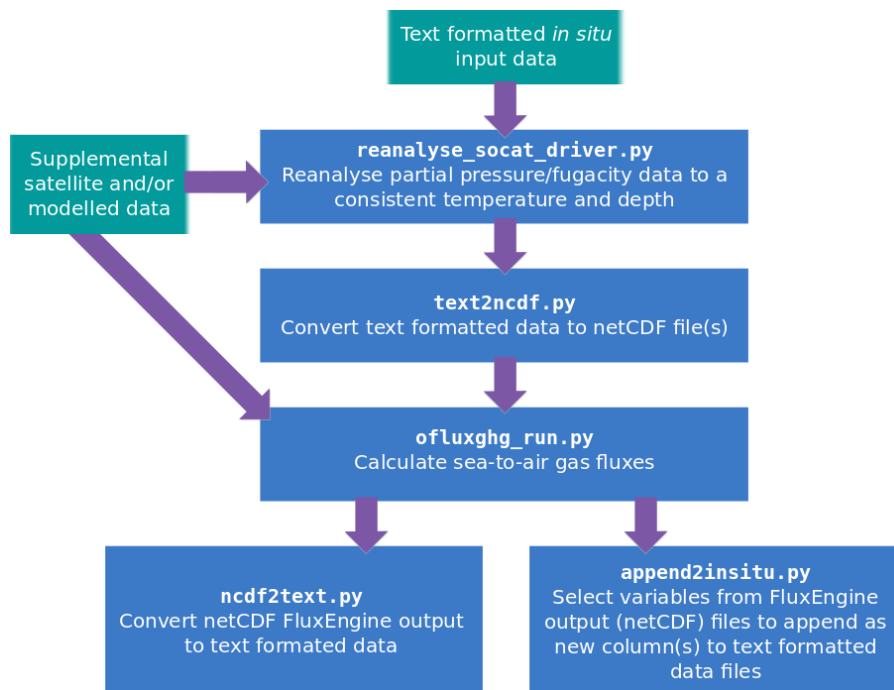


Figure 2: A typical CO₂ workflow for using FluxEngine with *in situ* data, showing the different utilities (blue boxes) and input data (green boxes) used at each stage.

2.4. Custom gas transfer velocity parameterisation

260 The processes that govern exchange, their relative importance and how gas exchange should be parameterised are all active areas of research. For example, a recent comparative study using FluxEngine highlighted a difference of up to 65% in global net CO₂ flux caused simply by using different wind-based gas transfer velocities (Wrobel and Piskozub, 2016).

265 FluxEngine has always allowed users to select or define different (mostly wind-based) transfer velocity parameterisations. However, version 3.0 adopts a modular approach to specifying the flux calculation, which makes it simpler for the user to extend the functionality and incorporate new gas transfer parameterisations. Custom parameterisations can be implemented as separate Python classes without modifying the core FluxEngine software. This is achieved by copying and modifying the template class provided in *rate_parameterisation.py*. Storing the new class within *rate_parameterisation.py* means
270 that the new parameterisation will be automatically incorporated into the toolkit ready to be selected in the configuration file for all users of the particular FluxEngine installation. These custom parameterisations can define new input variables and therefore make use of additional input data files that can be included in the configuration file and will be automatically loaded into memory without requiring any additional setup. These custom parameterisations can also produce new data layers in the
275 final netCDF output, such as the results from intermediate calculation steps, which may be useful for testing or subsequent analysis outside of FluxEngine. Examples of how to use this functionality are provided in the source code. The toolbox documentation describes the process of, and best practices for, extending FluxEngine in this way (see Sect. 9.1 and 9.2 within *FluxEngineV3_instructions.pdf*).



280 This increased flexibility means that users can define and use region-specific gas transfer
parameterisations or incorporate new transfer processes into existing gas transfer parameterisations
(such as the impact of biological surfactants as discussed by Pereira *et al.*, 2018). Case studies one
(Sect. 3.1) and two (Sect. 3.2) demonstrate the use of different gas transfer parameterisations, while
285 which is used to assess the impact of biological surfactants on the N₂O gas fluxes. Case study four
(Sect 3.4) utilises a gas transfer velocity parameterisation that uses turbulent kinetic energy dissipation
and provides an example of using additional input data.

2.5. Extensions for other sparingly soluble gases

290 The toolbox now supports the handling of two other sparingly soluble gases, (CH₄ and N₂O), and so
gas specific data can be substituted into Eq. (1) or Eq. (2) (dependent upon the choice of setup). Gas
specific parameterisations for Schmidt number (Sc) and solubility (α) are automatically chosen from
those provided in Wanninkhof, 2014. The option to use the older Sc and solubility parameterisations
295 from Wanninkhof, 1992 is also included for compatibility with previous versions and to aid
comparative analysis. It is worth noting that both sets of Sc parameterisations are only valid for salt
water (35 PSU), and care should be taken when using them for analysis of freshwater data, or regions
with lower salinity (e.g. the Baltic Sea, see case study two, Sect. 3.2). Support for additional and user-
defined Schmidt number parameterisations are likely to be added in the future. FluxEngine can
300 calculate dissolved gas concentration from the gas input data, which can be supplied as either partial
pressure or mean molar fraction of a gas in the dry atmosphere. Alternatively, dissolved gas
concentrations can be provided directly as an input.

3. Case study examples of the new capabilities

305 The following sections describe the application and results from four case studies that illustrate the new
capabilities. Table 1 summarises the new features that are demonstrated in each case study. The
respective configuration file for each case study can be accessed via the FluxEngine GitHub repository
(<http://github.com/oceanflux-ghg/FluxEngine>).

	New features utilised
Case study 1: Calculating sea to air CO ₂ gas fluxes from research cruise data	Flexible input data specification to select <i>in situ</i> data files and unit conversion using pre-processing functions (Sect. 2.2). Utilises new support for <i>in situ</i> data analysis, including the use of the <i>text2ncdf.py</i> and <i>append2insitu.py</i> tools, custom temporal resolution, reanalysis of fCO ₂ to a consistent temperature field.
Case study 2: calculating sea to air CO ₂ gas fluxes from Östergarnsholm fixed station data.	Flexible input data specification to select <i>in situ</i> data files and unit conversion using pre-processing functions (Sect. 2.2).



	Utilises new support for <i>in situ</i> data analysis, including use of <code>text2ncdf.py</code> , daily temporal resolution, use of the reanalysis tool and output formatted as time-series (Sect. 2.3).
Case study 3: Surfactant suppression of sea to air N ₂ O gas fluxes using the MEMENTO database.	<p>Flexible input data specification and unit conversion using pre-processing functions (Sect 2.2).</p> <p>Utilises new support for <i>in situ</i> data analysis, including use of the <code>text2netcdf.py</code> and <code>append2insit.py</code> tools, custom temporal resolution and cruise-specific time interval (Sect. 2.3).</p> <p>Custom gas transfer parameterisation (Sect. 2.4).</p> <p>Calculation of N₂O gas fluxes (Sect. 2.5).</p>
Case study 4: Gas transfer velocity parameterisation using turbulent kinetic energy dissipation rate.	<p>Unit conversion and use of custom pre-processing functions to calculate the dissipation rate from the input data. This uses the pre-processing functions to perform a non-trivial computation (Sect. 2.2).</p> <p>Use of a custom gas transfer parameterisation which includes the specification of an additional input data layer (Sect. 2.4).</p>

Table 1: Summary of the new functionality demonstrated in each research case study.

310

3.1 Case study 1: Calculating CO₂ fluxes from research cruise data

Each year over 1 million new *in situ* data points are included within the annual updates to the SOCAT dataset. Field scientists collecting these data often need to calculate the coincident sea-to-air gas fluxes, either using solely *in situ* measurements or through combining them with satellite Earth observation and/or model data.

315

Here we illustrate the procedure for calculating sea-to-air gas fluxes from *in situ* data collected during four different sampling campaigns. These *in situ* data (Kitidis and Brown, 2017; Schuster, 2016; Steinhoff *et al.*, 2016; Wanninkhof *et al.*, 2016) were all collected in the north Atlantic during October 2013. For convenience these are referred to as cruises 1-4, respectively. The *in situ* data were first downloaded from PANGAEA (an open access data publishing and archiving repository) in tab-delimited format. The datasets follow the standard SOCAT structure and content (see Bakker *et al.*, 2016 table 9) and so they include sea surface temperature, salinity, surface air pressure, and fugacity of CO₂ in the seawater (fCO₂).

320



325

The majority of the measurements needed for the sea-to-air CO₂ gas flux calculation were measured *in situ* and exist within the downloaded datasets. However, wind speed (for the gas transfer parameterisation) was missing in all cases. Therefore to complement these *in situ* data, multi-sensor merged wind speed data at 10 m were downloaded (Cross-Calibrated Multi-Platform, CCMPv2, 6 hour temporal resolution, 0.25° × 0.25° spatial grid (Atlas, *et al.*, 2011)). These wind speed data were appended to the *in situ* data by matching each *in situ* measurement to the closest temporal and spatial grid point. This same process was used to add columns for the second and third moments of wind speed, which were estimated by taking the second and third power of wind speed, respectively.

330

335

Two datasets (Schuster, 2016; Steinhoff, *et al.*, 2016) were missing molar fraction of CO₂ in dry air (xCO₂) data, and so the same method of matching temporal and spatial grid points was used to fill in these fields using the GLOBALVIEW CO₂ dataset from the US National Oceanic and Atmospheric Administration (NOAA) Earth System Research Laboratory (ESRL) (GLOBALVIEW-CO₂, 2013). For ease, these additional wind speed and xCO₂ data were downloaded, extracted and then inserted into the tab delimited *in situ* file using some simple custom python scripts but the same process could be performed manually. These scripts are not part of FluxEngine but the functionality they provide will likely be available as part of the planned interactive Jupyter tutorials, see Sect. 4.

340

345

The *in situ* data were collected from different ships and underway systems, all sampling water at different and unknown depths. These measurements are typically collected from a few metres below the water surface, whereas the CO₂ concentration (combination of fCO₂ and solubility) either side of the mass boundary layer is required for an accurate gas flux calculation. Before these data from multiple sources can be used for an accurate gas flux calculation, they need to be reanalysed to a common temperature dataset and depth (Goddijn-Murphy *et al.*, 2015; Woolf *et al.*, 2016). Therefore the *reanalyse_socat_driver.py* tool was first used to reanalyse all fCO₂ data to a consistent temperature and depth.

350

355

In the absence of coincident *in situ* skin (or sub-skin) temperature data, the slow re-equilibrium time of CO₂ in seawater (i.e. on the order of months for CO₂ to equilibrate with the atmosphere) ensure that monthly mean, or rolling monthly mean (centred on the day of interest) skin or sub-skin sea surface temperature (SST) values are suitable for re-analysing the *in situ* data. Arguably a robust daily skin or sub-skin SST value would be better, even if that is obtained by a seasonal curve fitted to the monthly values and interpolated to the day of interest. Here for simplicity monthly mean sea surface temperatures from the Reynolds Optimally Interpolated Sea Surface Temperature dataset (OISST, Reynolds *et al.*, 2007) were used as the reference subskin temperature dataset, resulting in reanalysed fCO₂ that are valid for the bottom of the mass boundary layer (termed sub-skin within Woolf *et al.*, 2016).

360

365

The reanalysed fCO₂ were then inserted into the tab-delimited *in situ* dataset producing a single dataset. The tab-delimited file was then converted into a netCDF format file using the *text2ncdf.py* tool. This tool groups all data according to a user-specified spatial sampling grid, calculating the mean value and standard deviation for each cell within the grid as well as the number of data that were used to calculate these statistics. Here, for simplicity, the spatial resolution was defined as 1° × 1° grid. FluxEngine was



then configured to use each of the variables in the resulting netCDF file as input, with a pre-processing
370 function applied to convert Reynolds OISST from Celsius to Kelvin (as all SST data within the main
flux calculation use Kelvin). In order to produce a single netCDF output file for the entire 35 day
period the temporal resolution for the flux calculation was set to 35 days. This allows the cruise tracks
from all four cruises (1-4) to be easily visualised at the same time.

375 The sea-to-air CO₂ fluxes were then calculated using the rapid model (see Eq. (1) and Woolf *et al.*,
2016) and was run using a quadratic wind speed based gas transfer velocity parameterisation (Ho *et al.*,
2007). To identify the impact of the fCO₂ reanalysis stage, the sea-to-air CO₂ flux calculation was
repeated using the original *in situ* fCO₂.

380 Figure 3a shows the resultant calculated CO₂ flux along each of the cruises (1-4). The southern sub-
tropical part of the cruise track 1 represents an area of the ocean that is a sink of CO₂ (negative sea-to-
air flux). The northern sub-tropical section of cruise 1 shows an overall positive CO₂ flux into the
atmosphere, while south of 15°N the net fluxes are smaller and in variable direction. The highest
magnitude fluxes were seen around the European continental shelf in cruise tracks 3 and 4, with a
385 strong ocean sink west of Ireland and an intermittent source of CO₂ in the North Sea. Figure 3b shows
the difference in calculated net flux between use of the original fCO₂ data and the reanalysed fCO₂.
Whilst very little difference is seen over large lengths of cruise tracks 1, 2 and 4, there are substantial
differences of >50% in some regions, for example within the frontal regions at the edge of the
European shelf seas (cruise track 3) or in the southern section of cruise track 1 where temporally and
390 spatially dynamic temperature gradients appear to exist. Interestingly, there are also examples (e.g.
along the equatorial part of cruise track 1 and the western part of cruise track 2) where the direction of
the flux has changed as a result of re-analysing the fCO₂ data.

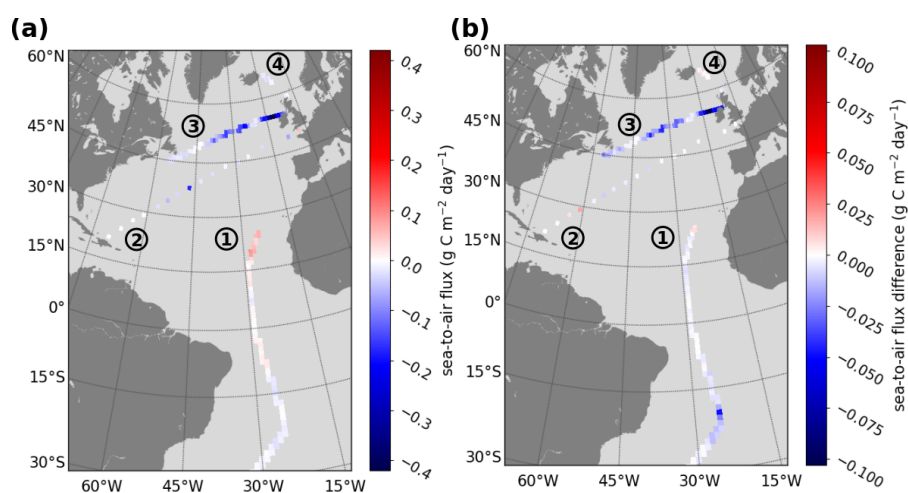


Figure 3: Example sea-to-air CO₂ fluxes calculated using *in situ* data and the gas transfer velocity detailed in (Ho *et al.*, 2007) (a) fluxes calculated for four sampling cruises in the North Atlantic during October and November 2013 (Kitidis and Brown, 2017; Schuster, 2016; Steinhoff *et al.*, 2016; Wanninkhof *et al.*, 2016) labelled 1-4, respectively. (b) The difference in the calculated flux resulting from using the reanalysed fCO₂



compared to the original *in situ* $f\text{CO}_2$ data (reanalysed minus original).

395

The `append2insitu.py` tool was then used to append FluxEngine output to the original input data file for the Kitidis and Brown (2017) dataset. The output from this tool enables the user to visualise FluxEngine output (including any additional input data such as the CCMP wind speed data) as a time series alongside all other measured *in situ* data. Figure 4 shows the time series of sea surface temperature, $f\text{CO}_2$, and $x\text{CO}_2$ (from the *in situ* data) alongside the corresponding CCMP wind speed and the calculated concentrations and fluxes using the original and reanalysed $f\text{CO}_2$ data.

400

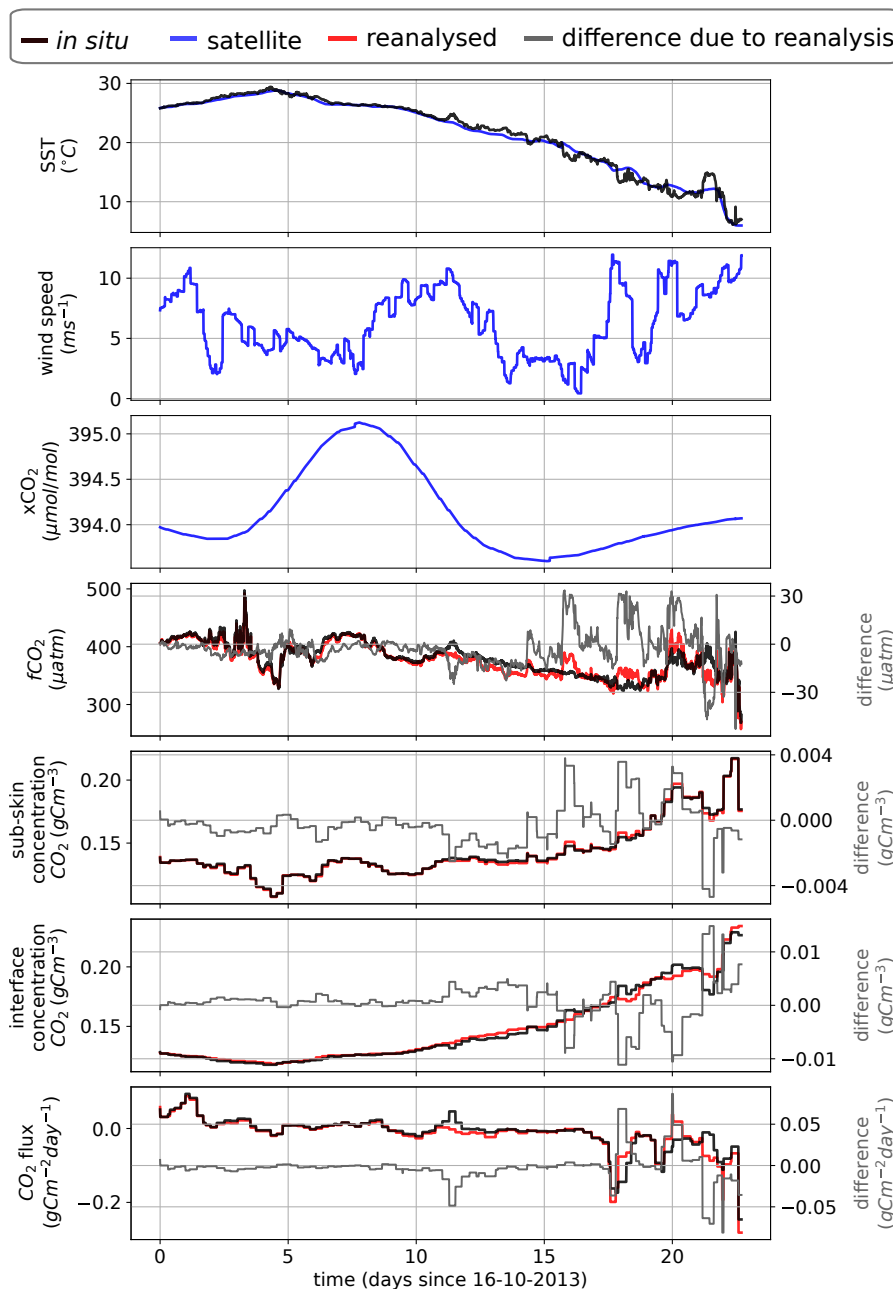


Figure 4: Time series of the (Kitidis and Brown, 2017) *in situ* campaign data with the sea-to-air CO_2 flux as



calculated by FluxEngine using the Ho *et al.*, (2006) gas transfer velocity parameterisation. The results from the reanalysed $f\text{CO}_2$ values are shown in red to distinguish them from the original data. The differences in $f\text{CO}_2$, sub-skin and interface CO_2 concentration and sea-to-air CO_2 flux, resulting from the reanalysis, are shown in grey (reanalysed minus original).

3.2 Case study 2: Calculating CO_2 fluxes from Östergarnsholm fixed station data

405 In this section the new capabilities for calculating gas fluxes from fixed stations is demonstrated using data from the long term monitoring station at Östergarnsholm. The Östergarnsholm station is situated in the Baltic Sea (57.42N, 18.99E) and is part of the Integrated Carbon Observation System (ICOS) infrastructure. The station was originally established in 1995 with the aim of collecting data on the marine atmospheric boundary layer to support research on the exchange of heat, momentum and CO_2
410 between the atmosphere and ocean. It is equipped with instruments to measure (amongst other parameters) profiles of wind speed, water temperature and aqueous $f\text{CO}_2$.

The new FluxEngine support for calculating gas fluxes from fixed stations uses the temporal dimension of the input files, creating output files of the same dimension that can be easily visualised as a time series. Data for the Östergarnsholm monitoring station covering a period from 28th January 2015 to the
415 9th September 2015 were downloaded from the data repository (Rutgersson, 2017). These data contain *in situ* measurements for $f\text{CO}_2$, salinity and temperature, model reanalysis air pressure at sea level from the National Center for Environmental Prediction, National Center for Atmospheric Research (NCEP/NCAR) dataset (Kalnay *et al.*, 1996), $x\text{CO}_2$ from the NOAA ESRL GLOBALVIEW dataset (GLOBALVIEW-CO2, 2013) and World Ocean Atlas salinity data (Boyer *et al.*, 2013). CCMP wind speed data were extracted and added to the tab delimited *in situ* dataset using the same method as used
420 in case study 1 (Sect. 3.1). For gridded input data a single grid point containing the Östergarnsholm station location was selected from a global $1^\circ \times 1^\circ$ projected grid.

425 The *text2ncdf.py* tool was configured to convert the text formatted data file into a single netCDF file using a temporal resolution of one day. This produced a netCDF file with a temporal dimension size of 246 (days), containing the daily mean value for each of the 246 days covered by the dataset. FluxEngine was configured to use this file as input, and to index into the temporal dimension appropriately. The $f\text{CO}_2$ data were reanalysed using the same method and data as used in case study 1
430 to determine $f\text{CO}_2$ at the bottom of the mass boundary layer.

The flux calculation used the rapid model (Woolf *et al.*, 2016) with the Nightingale *et al.* (2000) wind based gas transfer velocity parameterisation and was performed separately using the reanalysed $f\text{CO}_2$ and original $f\text{CO}_2$ data. The temporal resolution was set to provide daily calculations for each of the
435 246 days allowing seasonal variations to be observed, but not diurnal variations. FluxEngine supports arbitrary temporal resolutions to within minute precision and the choice predominantly depends on the resolution of the available data and the particular research questions to be addressed. FluxEngine was configured to write output into a single netCDF file as a time series. Figure 5 shows the time series of SST, wind speed, $x\text{CO}_2$, $f\text{CO}_2$, concentration of CO_2 and calculated sea-to-air CO_2 flux. FluxEngine output produced by using the reanalysed $f\text{CO}_2$ are plotted in red. There was a mean increase of $0.022 \text{ g C m}^{-2} \text{ day}^{-1}$ in sea to air CO_2 flux (a 35% increase in outgassing) when using the reanalysed $f\text{CO}_2$.
440

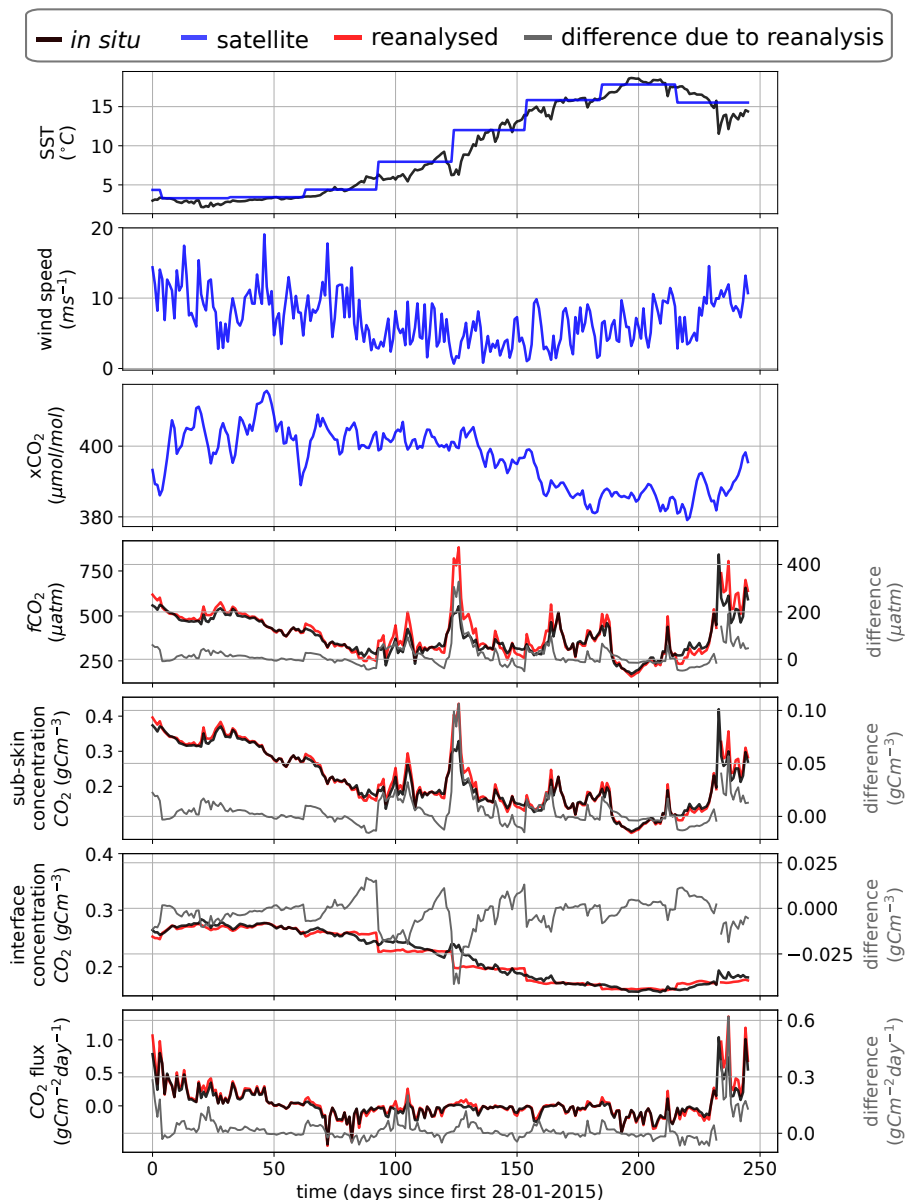


Figure 5: FluxEngine output file using data from Östergarnsholm station over the 246 day period. Example components of the sea-to-air flux calculation are shown alongside the calculated CO₂ flux for fCO₂ reanalysed to a consistent temperature and depth and unprocessed fCO₂ data. The differences in fCO₂, sub-skin and interface CO₂ concentration and sea-to-air CO₂ flux, resulting from the reanalysis, are shown in grey (reanalysed minus original).

3.3 Case study 3: Surfactant suppression of N₂O gas fluxes using the MEMENTO database

445

Nitrous oxide (N₂O) and methane (CH₄) are both climatically important gases. In the troposphere, they act as greenhouse gases (IPCC, 2013), whereas stratospheric N₂O is the major source for NO radicals which are involved in one of the main ozone reaction cycles (Ravishankara *et al.*, 2009). Source estimates indicate that the world's oceans play a major role in the global budget of atmospheric N₂O and a minor role in the case of CH₄ (IPCC, 2013). Oligotrophic ocean areas are near equilibrium with



the atmosphere and, consequently, make only a relatively small contribution to overall oceanic
450 emissions, whereas biologically productive regions (e.g., estuaries, shelf and coastal upwelling areas)
appear to be responsible for the major fraction of the N₂O and CH₄ emissions (Bakker *et al.*, 2014).

Surfactants are surface-active compounds that can suppress turbulence at the sea surface thus altering
air-sea gas exchange (McKenna and Bock, 2006; Pereira *et al.*, 2016; Salter *et al.*, 2011). There is
455 growing evidence from field and laboratory studies that naturally occurring surfactants can
significantly reduce the flux of N₂O across the water/atmosphere interface (Kock *et al.*, 2012;
Mesarchaki *et al.*, 2015).

Previous work, which studied CO₂ fluxes, found that surfactants potentially reduce the annual net
460 integrated CO₂ flux by up to 9% in the Atlantic Ocean (Pereira *et al.*, 2018). Here, we use FluxEngine
to apply the methodology of Pereira *et al.*, (2018) to *in situ* data from the MEMENTO (MarinE
MethanE and NiTrous Oxide) database (Kock and Bange, 2015) in order to estimate the equivalent
suppression effect on the exchange of N₂O between ocean and atmosphere.

465 While FluxEngine is able to calculate sea-to-air fluxes of both N₂O and CH₄, we confined our analysis
to N₂O because of the sparsity of CH₄ data. *In situ* and 1° x 1° gridded monthly mean atmospheric and
ocean partial pressure of N₂O, sea surface temperature and salinity were obtained from the MEMENTO
database for the Atlantic Meridional Transect (AMT) cruise (AMT-24, JR303), which took place
between September and November 2014 (Brown and Rees, 2018). These data were supplemented with
470 Earth observation wind speed, U_{10} , from the CCMP dataset and modelled air pressure from the
European Centre for Medium-Range Weather Forecasts (ECMWF). All input data were gridded to
monthly means with a 1° x 1° resolution. While sea surface temperature measured from pumped water
samples collected at some depth are used here, recent AMT cruises (from 2016) have included an
Infrared Sea Surface Temperature Autonomous Radiometer (ISAR) (Donlon *et al.*, 2008) and therefore
475 future AMT datasets will include direct sea skin temperature measurements. Using skin temperature
measurements are likely to further increase the accuracy of the flux calculation.

A custom gas transfer velocity parameterisation was implemented following the template provided in
the toolbox to calculate the gas transfer suppression due to biological surfactants in surface waters. This
480 parameterisation uses the gas transfer velocity of (Nightingale *et al.*, 2000) combined with an estimate
of the degree of surfactant suppression from (Pereira *et al.*, 2018). FluxEngine was configured to use
the rapid flux model (Woolf *et al.*, 2016) and run once with the standard Nightingale *et al.*, (2000) gas
transfer parameterisation (no suppression case) and then again using the Pereira *et al.*, (2018)
parameterisation (suppression case). This new gas transfer parameterisation is now freely available
485 within the FluxEngine (and can be selected by specifying
`k_Nightingale2000_with_surfactant_suppression` for the `k_parameterisation` option).

The calculated sea-to-air N₂O flux for each grid cell (within which at least one *in situ* measurement
exists) are shown in Fig. 6a, while the difference in sea-to-air flux due to surfactant suppression is
490 shown in Fig. 6b. The largest fluxes in both directions occur in the tropics and sub-tropical part of the
AMT cruise track (Fig. 6a). Suppression of the gas transfer reduces the magnitude of the air-sea flux



(regardless of direction of flux) and the largest absolute suppression is seen in the tropics and sub-tropical part of both (Fig. 6a and Fig. 6b).

- 495 The *append2insitu.py* utility was used to combine FluxEngine output with the original *in situ* data. The time series are shown in Fig. 6c for SST, wind speed, atmospheric and aqueous N₂O, and sea-to-air N₂O flux. The net fluxes along the transect are generally small and in both directions. The overall mean flux was negative but small, $-2.4 \times 10^{-3} \pm 2.5 \times 10^{-2} \text{ g N}_2\text{O m}^{-2} \text{ day}^{-1}$ (no suppression) and $-1.9 \times 10^{-3} (\pm 2.0 \times 10^{-2}) \text{ g N}_2\text{O m}^{-2} \text{ day}^{-1}$ (suppression), indicating in both cases a small net flux into the ocean.
- 500 There was a mean flux suppression due to surfactants of 13% for the entire dataset, while there was an overall (net) change in flux of -20% (reducing the flux to the ocean).

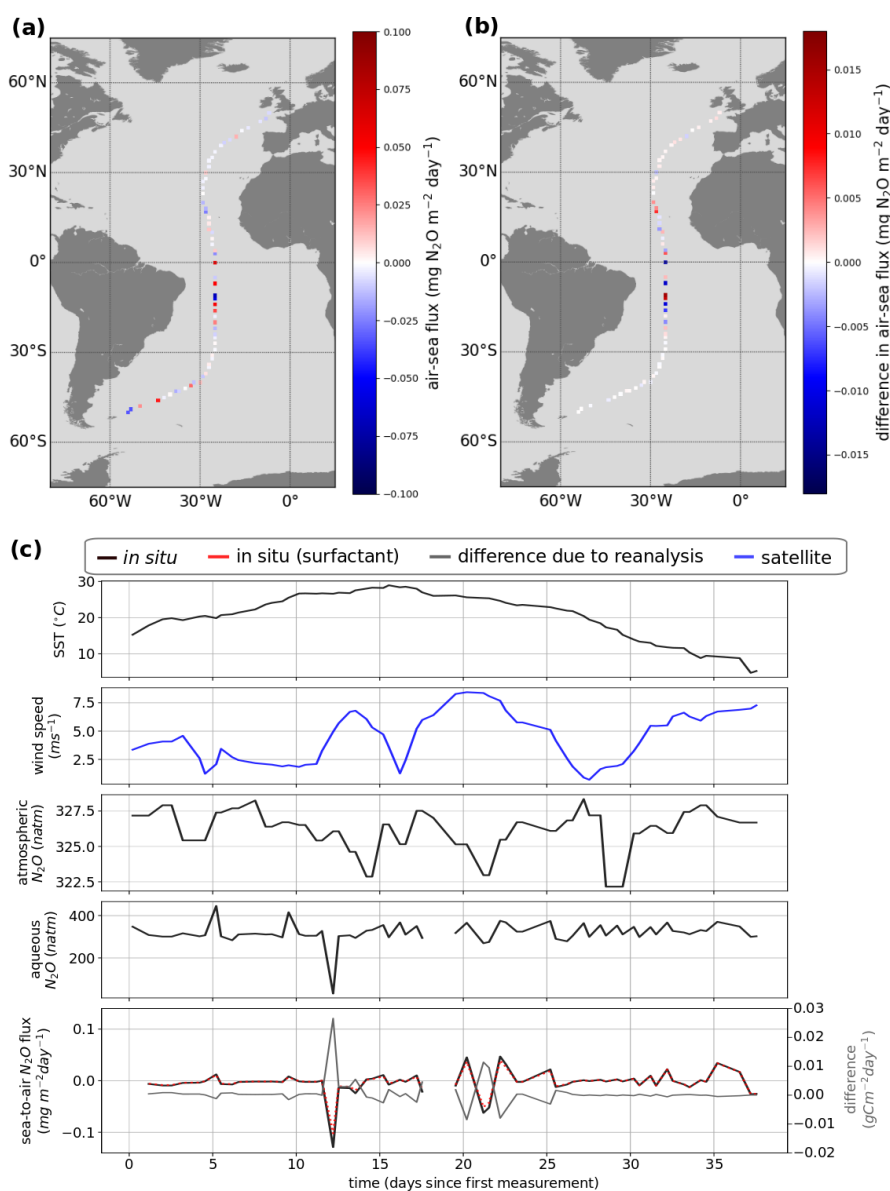




Figure 6: (a) N₂O sea-to-air N₂O flux taking into account surfactant suppression. (b) Change in N₂O flux resulting from surfactant suppression. (c) Time series of SST, wind speed, atmospheric N₂O, aqueous N₂O and sea-to-air flux.

3.4 Case study 4: Gas transfer velocity parameterisation using turbulent kinetic energy dissipation rate

505 The gas transfer velocity, k in equation 1 and 2, is determined by the turbulent mixing near the ocean surface (Jähne *et al.*, 1987). While it is common to estimate gas transfer using a polynomial relationship with wind speed, turbulence in the upper ocean is influenced by additional physical processes which are independent or not solely dependent on the wind. These include wave breaking, shear stress due to geostrophic currents, wind-wave-current interactions, bottom-generated turbulence, 510 tidal forces and precipitation (Villas Boas *et al.*, 2019; Zappa *et al.*, 2007; Zhao *et al.*, 2018).

In this case study we apply a turbulent kinetic energy dissipation rate (ϵ) based gas transfer velocity parameterisation, as developed by Zappa *et al.* (2007), to quantify the impact of wind- and wave-driven turbulence on sea-to-air CO₂. Zappa *et al.* used direct measurements of k and ϵ in aquatic and shallow 515 marine regions to derive the following relationship

$$k = 0.419Sc^{-0.5}(\epsilon\nu)^{0.25} \quad (3)$$

where k is the gas transfer velocity ($m\ s^{-1}$), Sc is the Schmidt number, ϵ is the turbulent kinetic energy 520 dissipation rate ($W\ kg^{-1}$) and ν is the kinematic viscosity of water ($m^2\ s^{-1}$). We calculate the monthly mean ϵ using the monthly mean wave (swell, secondary swell and wind waves) to ocean turbulent kinetic energy flux (FOC) provided by the WAVEWATCH III model re-analysis (WAVEWATCH III development group, 2016). The mean dissipation rate of turbulent kinetic energy, ϵ_{mean} , is calculated using $\epsilon_{mean} = FOC / (\rho z_{max})$, where ρ is the density of sea water (taken to be $1026\ kg\ m^{-3}$) and z_{max} is 525 the maximum depth over which dissipation is assumed to occur (taken as 10 m from Fig. 8 of Craig and Banner, 1994). This provides the mean total dissipation rate through the volume of water. Equation 3 is valid for ϵ measurements near the surface (of the order of 0.1 to 0.2 m) and ϵ is known to decrease exponentially with depth. To estimate ϵ at a depth of 0.2 m we first fit an exponential function to the curve of ϵ from fig 8 of Craig and Banner (1994) which gave:

$$\epsilon = \beta \exp(0.20z + 0.78) \quad (4)$$

where z is depth and $\beta=1.86 \times 10^{-3}$. Normalising this function to have a mean ϵ equal to ϵ_{mean} allows ϵ at any depth to be determined. This was done by fitting β to minimise the difference between ϵ_{mean} 535 calculated from FOC and ϵ_{mean} calculated from equation 4 to produce separate depth relationships with ϵ for each individual grid cell. Finally, the dissipation rate at 0.2 m was calculated by substituting $z=0.2$ into the final depth relationship. The process of fitting of the depth relationship and calculating ϵ at depth $z=0.2$ was implemented using a custom pre-processing function that is included as an example in the FluxEngine download. This demonstrates how pre-processing functions can be used to perform 540 complex data processing.



FluxEngine was then used to calculate monthly sea-to-air CO₂ fluxes, globally, for 2010. All inputs to FluxEngine were provided as monthly averages with a 1° x 1° resolution. The other input data were
545 wind speed data from WAVEWATCH III re-analysis forcing field (WAVEWATCH III development
group, 2016), sea surface temperature from Reynolds Optimally Interpolated Sea Surface Temperature
dataset (OISST, Reynolds *et al.*, 2007), salinity data from the NOAA World Ocean Atlas (Zweng *et al.*,
2018), atmospheric molar fraction of CO₂ in dry air data from the GLOBALVIEW CO₂ dataset
(GLOBALVIEW-CO₂, 2013), and fCO₂ data from the SOCAT derived sea-to-air CO₂ flux reference
550 dataset for 2010 (Woolf *et al.*, in-review). Since the Zappa *et al.*, (2007) relationship was parameterised
in low to moderate wind speeds and in shallow marine environments, a mask was set in the
configuration file to constrain the calculation to grid cells with wind speeds less than 10 m s⁻¹ and shelf
sea water depths between than 20 m and 200, and 20 and 500 m. These depth ranges were chosen to be
consistent with previous studies (e.g. Laruelle *et al.*, 2018; Shutler *et al.*, 2016).

555 The *ofluxghg_flux_budgets.py* tool was used to compute the annual integrated net sea-to-air flux in all
shelf sea regions. Collectively the global shelf seas result in a net integrated flux into the ocean (sink)
of 0.57 to 0.78 Pg C for 2010, where the range is due to the two shelf definitions. These results are
within the bounds of those determined by previous studies (0.2 – 1 PgC yr⁻¹ from Laruelle *et al.*, 2018;
Laruelle *et al.*, 2016). However we note that all previous studies have used wind speed for calculating
560 gas exchange. Repeating the analysis with a wind speed based gas transfer velocity (Wanninkhof *et al.*,
2014) instead of equation 4 gives an ~8% smaller net integrated flux of 0.53 to 0.72 Pg C. This result
could suggest that published values of the global shelf sea CO₂ sink (calculated using wind speed gas
transfer) are underestimated, as they do not fully account for wind-wave-current interactions and
whitcapping. Figure 7 shows the resulting mean annual sea-to-air CO₂ flux in 2010 for global shelf
565 seas. The FluxEngine has the capability to use non-wind driven gas transfer parameterisations allowing
more physically based approaches to be evaluated such as the use of ϵ . The first synoptic-scale
observation-based estimates of ϵ could soon be possible from space using Doppler techniques (e.g.
Ardhuin *et al.*, 2019).

570

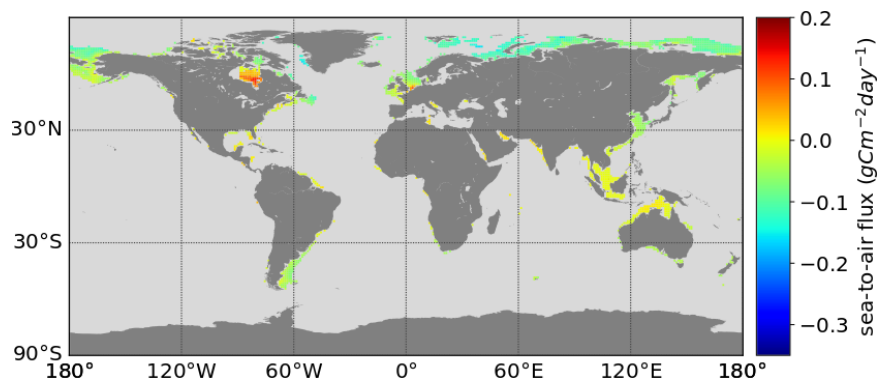


Figure 7: Mean sea-to-air CO₂ flux of shelf seas in 2010 using the Zappa *et al.*, (2007) gas transfer relationship for all regions and months with wind speeds 0 to 10 m s⁻¹. Shelf regions are defined as having depth between 20 m and 200 m.

4. Future developments



The FluxEngine toolbox will continue to be developed in response to new advances in research. To increase user-uptake future work will include a series of iPython Jupyter notebooks. These online and interactive iPython notebooks will allow users to investigate the toolbox without the need to install any software. Users will be able to modify and re-run the notebook and immediately see the impact of any changes. This approach has been previously used for supporting collaborative research and summer school teaching. For example, Jupyter notebooks could be used to provide worked examples of: i) simple execution using custom input data ii) pre-processing of *in situ* data, iii) creating and testing custom gas transfer parameterisations and pre-processing functions, iv) driving FluxEngine with a custom python script to perform a sensitivity analysis, or v) using the verification tools module to verify custom changes and extensions to the toolbox.

5. Conclusions

The FluxEngine is an open-source and freely available software toolbox that provides standardised and verified calculations of gas exchange and net integrated fluxes between the ocean and atmosphere, and the toolbox is now being used by *in situ*, Earth observation and modelling scientific communities. The development of the toolbox was driven by the desire to reduce duplication of effort, to facilitate collaboration between different research communities, and thus to accelerate advancements in air-sea gas flux research and monitoring.

Building on Shutler *et al.* (2016), which demonstrated the toolbox and verified the accuracy of the calculations, this paper demonstrates new capabilities that considerably broadens the scope of research questions that can be addressed using FluxEngine. Version 3.0 can now be easily installed and executed on a desktop or laptop computer and does not require specialist hardware or software libraries. It can be used as a python library or as a set of stand-alone command line utilities. The toolbox now includes an extensive suite of tools for calculating gas fluxes directly from *in situ* data. Collectively these improvements have streamlined the process for extending the toolbox and will allow users to easily take advantage of newly developed gas transfer velocity parameterisations and/or new sources of input data. These new tools and the toolbox are fully compatible with the internationally agreed data structures being used by the SOCAT and the MEMENTO communities.

The inclusion of the handling of CH₄ and N₂O sea-air gas fluxes is intended to directly support those communities studying these gases. Significant international research focus and effort is now being directed to collating data on these gases towards monitoring and understanding their spatial distribution and variability.

FluxEngine will continue to be updated as new approaches become available. Further development will be guided by the needs of the international research and monitoring communities, and so we welcome feedback from users on all aspects of the toolbox.

Code availability

The FluxEngine software is open source and available on a creative commons license via <http://github.com/oceanflux-ghg/FluxEngine>

615



6. Appendix A: Utility names and descriptions

Several additional utilities are provided as Python scripts to support the installation, verification, execution and processing of output (these are listed in table 2).

Utility	Description
<i>append2insitu.py</i>	Appends netCDF data (e.g. FluxEngine output) to text formatted data files as new columns. Matching rows by longitude, latitude and time.
<i>install_dependencies_macos.py</i> , <i>install_dependencies_ubuntu.py</i>	Installation scripts. Installation instructions are provided for Windows users in <i>FluxEngineV3_instructions.pdf</i>
<i>ncdf2text.py</i>	Converts netCDF output files to text formatted files.
<i>ofluxghg_flux_budgets.py</i>	Calculates total monthly and annual gas flux from FluxEngine output. Supports global and regional analysis.
<i>ofluxghg_run.py</i> <i>reanalyse_socat_driver.py</i>	Commandline tool used to run FluxEngine Uses satellite sea surface temperature to reanalyse CO ₂ fugacity and partial pressure data to a consistent temperature and depth (see Goddijn-Murphy <i>et al.</i> , 2015)
<i>run_full_verification.py</i>	Runs an extended verification procedure. Required additional data from (Holding <i>et al.</i> , 2018)
<i>text2ncdf.py</i>	Converts text formatted data files into FluxEngine compatible netCDF format.
<i>validation_tools.py</i> , <i>compare_net_budgets.py</i>	Contains Python functions to aid verification of FluxEngine output to a reference dataset.
<i>verify_socatv4_sst_salinity_gradients_N00.py</i> , <i>verify_takahashi09.py</i>	Verifies that FluxEngine has been installed correctly by comparing output with a reference data from SOCAT-derived or Takahashi climatologies, respectively.

620 **Table 2:** Description of the bundled tools and scripts that are included in FluxEngine. Each tool can be used as a stand-alone command line tool or used as a Python package.

625 7. Appendix B: Datasets used

Table 3 provides details of each of the data sets that were used in the case studies.

Name	Parameter(s)	Reference/source
CCMP v2 (Cross-Calibrated Multi-Platform)	U ₁₀ (wind speed at 10m)	Atlas <i>et al.</i> , 2011 http://www.remss.com/measurements/ccmp/
OISST (Optimally-Interpolated Seas Surface Temperature)	Sea surface temperature (SST)	Reynolds <i>et al.</i> , 2007 https://www.ncdc.noaa.gov/oisst
GLOBALVIEW CO ₂	xCO ₂ (molar fraction of CO ₂ in dry air)	GLOBALVIEW-CO ₂ , 2013 https://www.esrl.noaa.gov/gmd/ccgg/globalview/co2/co2_intro.html
National Centers for Environmental Prediction, National Center for	Air pressure	Kalnay <i>et al.</i> , 1996 https://www.esrl.noaa.gov/psd/data/gridded/data.ncep.reanalysis.pressure.html



Atmospheric Research (NCEP/NCAR)		
Underway data from the James Clark cruise (74JC20131009)	SST, salinity, air pressure, fCO ₂	Kitidis and Brown, 2017 https://doi.pangaea.de/10.1594/PANGAEA.878492
Underway data from the Belguela Stream cruise (642B20131005)	SST, salinity, air pressure, fCO ₂	Schuster, 2016 https://doi.org/10.1594/PANGAEA.852980
Underway data from the Atlantic Companion cruise (77CN20131004)	SST, salinity, air pressure, fCO ₂	Steinhoff <i>et al.</i> , 2016 https://doi.org/10.1594/PANGAEA.852786
Underway data from the REYJAFOSS cruise (64RJ20131017)	SST, salinity, air pressure, fCO ₂ , xCO ₂	Wanninkhof <i>et al.</i> , 2016 https://doi.org/10.1594/PANGAEA.866092
Östergarnsholm station (77FS20150128)	Air pressure, salinity, SST, xCO ₂ (air), fCO ₂ (water)	Rutgersson, 2017 https://doi.pangaea.de/10.1594/PANGAEA.878531
MarinE MethanE and NiTrous Oxide database (MEMENTO)	SST, pN ₂ O _{air} , pN ₂ O _{water}	Kock and Bange, 2015 https://memento.geomar.de/
National Oceanic and Atmospheric Administration, US (NOAA) WAVEWATCH III	U ₁₀ (wind speed at 10m), FOC (wave to turbulent kinetic energy)	WAVEWATCH III development group, 2016

Table 3: The Earth observation *in situ*, model and climatology data used in this research.

Author contributions

630 Design and analysis performed by T. Holding, I. Ashton and J. Shutler. Software engineering performed by T. Holding and I. Ashton. Pre-processing of nitrous oxide data performed by A. Kock. All authors contributed to the preparation of the manuscript.

Acknowledgements

635 This work was partially funded by the European Space Agency (ESA) Support to Science Element (STSE) through the OceanFlux Greenhouse Gases project (contract 4000104762/11/I-AM), the OceanFlux Greenhouse Gases Evolution project (contract 4000112091/14/I-LG), and by the European Space Agency (ESA) through the Sea surface Kinematics Multiscale monitoring (SKIM) Mission Science study (contract 4000124734/18/NL/CT/gp) and the ESA SKIM Scientific Performance
 640 Evaluation study (contract 4000124521/18/NL/CT/gp), as well as through the NERC RAGNARoCC project, (grant ref. NE/K002473/1). Further development of FluxEngine was funded by the European Union's Seventh Programme for Research and Technology Development (grant no. 03FO773A (BONUS INTEGRAL) and grant no. 730944 (RINGO)).



645 The Surface Ocean CO₂ Atlas (SOCAT) is an international effort, endorsed by the International Ocean Carbon Coordination Project (IOCCP), the Surface Ocean Lower Atmosphere Study (SOLAS) and the Integrated Marine Biosphere Research (IMBeR) program, to deliver a uniformly quality-controlled surface ocean CO₂ database. The many researchers and funding agencies responsible for the collection of data and quality control are thanked for their contributions to SOCAT.

650 CCMP Version-2.0 vector wind analyses are produced by Remote Sensing Systems (<http://www.remss.com>). NCEP Reanalysis data provided by the NOAA/OAR/ESRL PSD, Boulder, Colorado, USA, from their web site at <https://www.esrl.noaa.gov/psd/>.

655 MEMENTO (<https://memento.geomar.de/>) is currently supported by the Kiel Data Management Team at GEOMAR and the BONUS INTEGRAL Project.

This study is a contribution to the international IMBeR project and was supported by the UK Natural Environment Research Council National Capability (CLASS Theme 1.2) funding to Plymouth Marine
660 Laboratory. This is contribution number 330 of the AMT programme.

BONUS INTEGRAL receives funding from BONUS (Art 185), funded jointly by the EU, the German Federal Ministry of Education and Research, the Swedish Research Council Formas, the Academy of Finland, the Polish National Centre for Research and Development, and the Estonian Research Council.

665 **Competing interests**

The authors declare that they have no conflict of interest.

670 References

Ardhuin, F., Aksenov, Y., Benetazzo, A., Bertino, L., Brandt, P., Caubet, E., Chapron, B., Collard, F., Cravatte, S., Delouis, J.-M., Dias, F., Dibarboure, G., Gaultier, L., Johannessen, J., Korosov, A., Manucharyan, G., Menemenlis, D., Menendez, M., Monnier, G., Mouche, A., Nougquier, F., Nurser, G., Rampal, P., Reniers, A., Rodriguez, E., Stopa, J., Tison, C., Ubelmann, C., van Sebille, E. and Xie, J.:

675 Measuring currents, ice drift, and waves from space: the Sea surface KInematics Multiscale monitoring (SKIM) concept, *Ocean Sci.*, 14(3), 337–354, doi:10.5194/os-14-337-2018, 2018.

Ardhuin, F., Brandt, P., Gaultier, L., Donlon, C., Battaglia, A., Boy, F., Casal, T., Chapron, B., Collard, F., Cravatte, S. E., Delouis, J., de Witte, E., Dibarboure, G., Engen, G., Johnsen, H., Lique, C., Lopez-Dekker, P., Maes, C., Martin, A., Marie, L., Menemenlis, D., Nougquier, F., Peureux, C., Ressler, G., Rio, M., Rommen, B., Shutler, J. D., Suess, M., Tsamados, M., Ubelmann, C., van Sebille, E., van der Vorst, M., Stammer, D. and Rampal, P.: SKIM, a candidate satellite mission exploring global ocean currents and waves. *Frontiers in Marine Science* (Accepted), 2019.

685 Ashton, I. G., Shutler, J. D., Land, P. E., Woolf, D. K. and Quartly, G. D.: A Sensitivity Analysis of the Impact of Rain on Regional and Global Sea-Air Fluxes of CO₂, edited by M. deCastro, *PLoS One*, 11(9), e0161105, doi:10.1371/journal.pone.0161105, 2016.



- 690 Atlas, R., Hoffman, R. N., Ardizzone, J., Leidner, S. M., Jusem, J. C., Smith, D. K. and Gombos, D.: A Cross-calibrated, Multiplatform Ocean Surface Wind Velocity Product for Meteorological and Oceanographic Applications, *Bull. Am. Meteorol. Soc.*, 92(2), 157–174, doi:10.1175/2010BAMS2946.1, 2011.
- 695 Bakker, D. C. E., Bange, H. W., Gruber, N., Johannessen, T., Upstill-Goddard, R. C., Borges, A. V., Delille, B., Löscher, C. R., Naqvi, S. W. A., Omar, A. M. and Santana-Casiano, J. M.: Air-Sea Interactions of Natural Long-Lived Greenhouse Gases (CO₂, N₂O, CH₄) in a Changing Climate, pp. 113–169, Springer, Berlin, Heidelberg., 2014.
- 700 Bakker, D. C. E., Pfeil, B., Landa, C. S., Metzl, N., O'Brien, K. M., Olsen, A., Smith, K., Cosca, C., Harasawa, S., Jones, S. D., Nakaoka, S., Nojiri, Y., Schuster, U., Steinhoff, T., Sweeney, C., Takahashi, T., Tilbrook, B., Wada, C., Wanninkhof, R., Alin, S. R., Balestrini, C. F., Barbero, L., Bates, N. R., Bianchi, A. A., Bonou, F., Boutin, J., Bozec, Y., Burger, E. F., Cai, W.-J., Castle, R. D., Chen, L., Chierici, M., Currie, K., Evans, W., Featherstone, C., Feely, R. A., Fransson, A., Goyet, C., Greenwood, N., Gregor, L., Hankin, S., Hardman-Mountford, N. J., Harlay, J., Hauck, J., Hoppema, M., Humphreys, M. P., Hunt, C. W., Huss, B., Ibáñez, J. S. P., Johannessen, T., Keeling, R., Kitidis, V., Körtzinger, A., Kozyr, A., Krasakopoulou, E., Kuwata, A., Landschützer, P., Lauvset, S. K., Lefèvre, N., Lo Monaco, C., Manke, A., Mathis, J. T., Merlivat, L., Millero, F. J., Monteiro, P. M. S., Munro, D. R., Murata, A., Newberger, T., Omar, A. M., Ono, T., Paterson, K., Pearce, D., Pierrot, D., Robbins, L. L., Saito, S., Salisbury, J., Schlitzer, R., Schneider, B., Schweitzer, R., Sieger, R., Skjelvan, I., Sullivan, K. F., Sutherland, S. C., Sutton, A. J., Tadokoro, K., Telszewski, M., Tuma, M., van Heuven, S. M. A. C., Vandemark, D., Ward, B., Watson, A. J. and Xu, S.: A multi-decade record of high-quality fCO₂ data in version 3 of the Surface Ocean CO₂ Atlas (SOCAT), *Earth Syst. Sci. Data*, 8(2), 383–413, doi:10.5194/essd-8-383-2016, 2016.
- 715 Boyer, T.P., J. I. Antonov, O. K. Baranova, C. Coleman, H. E. Garcia, A. Grodsky, D. R. Johnson, R. A. Locarnini, A. V. Mishonov, T.D. O'Brien, C.R. Paver, J.R. Reagan, D. Seidov, I. V. Smolyar, and M. M. Z.: World Ocean Database 2013, NOAA Atlas NESDIF, 72, 209, doi:10.7289/V5NZ85MT, 2013.
- 720 Brown, I. and Rees, A.: Nitrous Oxide measurements from CTD collected depth profiles along a North-South transect in the Atlantic Ocean on cruise JR303/AMT24/JR20140922, *Br. Oceanogr. Data Cent. - Nat. Environ. Res. Council. UK*, doi:10.5285/7cbed206-c122-2777-e053-6c86abc041f9, 2018.
- 725 Craig, P. D., Banner, M. L. and Craig, P. D.: Modeling Wave-Enhanced Turbulence in the Ocean Surface Layer, *J. Phys. Oceanogr.*, 24(12), 2546–2559, doi:10.1175/1520-0485(1994)024<2546:MWETIT>2.0.CO;2, 1994.
- 730 Donlon, C., Robinson, I. S., Wimmer, W., Fisher, G., Reynolds, M., Edwards, R. and Nightingale, T. J.: An Infrared Sea Surface Temperature Autonomous Radiometer (ISAR) for Deployment aboard Volunteer Observing Ships (VOS), *J. Atmos. Ocean. Technol.*, 25(1), 93–113, doi:10.1175/2007JTECHO505.1, 2008.



- 735 GLOBALVIEW-CO2: Cooperative Global Atmospheric Data Integration Project. 2013, updated annually. Multi-laboratory compilation of synchronized and gap-filled atmospheric carbon dioxide records for the period 1979-2012 (obspack_co2_1_GLOBALVIEW-CO2_2013_v1.0.4_2013-12-23), Compil. by NOAA Glob. Monit. Devision, doi:10.3334/OBSPACK/1002, 2013.
- 740 Goddijn-Murphy, L. M., Woolf, D. K., Land, P. E., Shutler, J. D. and Donlon, C.: The OceanFlux Greenhouse Gases methodology for deriving a sea surface climatology of CO2 fugacity in support of air–sea gas flux studies, *Ocean Sci.*, 11(4), 519–541, doi:10.5194/os-11-519-2015, 2015.
- 745 Henson, S. A., Humphreys, M. P., Land, P. E., Shutler, J. D., Goddijn-Murphy, L. and Warren, M.: Controls on open-ocean North Atlantic $\Delta p\text{CO}_2$ at seasonal and interannual timescales are different, *Geophys. Res. Lett.*, 45(17), 9067–9076, doi:10.1029/2018GL078797, 2018.
- Ho, D. T., Law, C. S., Smith, M. J., Schlosser, P., Harvey, M. and Hill, P.: Measurements of air-sea gas exchange at high wind speeds in the Southern Ocean: Implications for global parameterizations, *Geophys. Res. Lett.*, 33(16), L16611, doi:10.1029/2006GL026817, 2006.
- 750 Ho, D. T., Veron, F., Harrison, E., Bliven, L. F., Scott, N. and McGillis, W. R.: The combined effect of rain and wind on air–water gas exchange: A feasibility study, *J. Mar. Syst.*, 66(1–4), 150–160, doi:10.1016/J.JMARSYS.2006.02.012, 2007.
- 755 Holding, Thomas; Ashton, Ian; Woolf, David K; Shutler, J. D.: FluxEngine v2.0 and v3.0 reference and verification data, PANGAEA, doi:10.1594/PANGAEA.890118, 2018.
- 760 IPCC: Climate Change 2013: The Physical Science Basis. Contribution of Working Group I to the Fifth Assessment Report of the Intergovernmental Panel on Climate Change, edited by V. B. and P. M. M. Stocker, T.F., D. Qin, G.-K. Plattner, M. Tignor, S.K. Allen, J. Boschung, A. Nauels, Y. Xia, Cambridge University Press, Cambridge, United Kingdom and New York, NY, USA, 1535 pp. [online]
- 765 Jähne, B., Münnich, K. O., Böisinger, R., Dutzi, A., Huber, W. and Libner, P.: On the parameters influencing air-water gas exchange, *J. Geophys. Res.*, 92(C2), 1937, doi:10.1029/JC092iC02p01937, 1987.
- 770 Kalnay, E., Kanamitsu, M., Kistler, R., Collins, W., Deaven, D., Gandin, L., Iredell, M., Saha, S., White, G., Woollen, J., Zhu, Y., Leetmaa, A., Reynolds, R., Chelliah, M., Ebisuzaki, W., Higgins, W., Janowiak, J., Mo, K. C., Ropelewski, C., Wang, J., Jenne, R., Joseph, D., Kalnay, E., Kanamitsu, M., Kistler, R., Collins, W., Deaven, D., Gandin, L., Iredell, M., Saha, S., White, G., Woollen, J., Zhu, Y., Chelliah, M., Ebisuzaki, W., Higgins, W., Janowiak, J., Mo, K. C., Ropelewski, C., Wang, J., Leetmaa, A., Reynolds, R., Jenne, R. and Joseph, D.: The NCEP/NCAR 40-Year Reanalysis Project, *Bull. Am. Meteorol. Soc.*, 77(3), 437–471, doi:10.1175/1520-0477(1996)077<0437:TNYRP>2.0.CO;2, 1996.
- 775 Kitidis, Vassilis; Brown, I.: Underway physical oceanography and carbon dioxide measurements during James Clark Ross cruise 74JC20131009, PANGAEA, doi:10.1594/PANGAEA.878492, 2017.



- Kock, A. and Bange, H.: Counting the Ocean's Greenhouse Gas Emissions, *Earth Sp. Sci. News*, 96, doi:10.1029/2015EO023665, 2015.
- 780 Kock, A., Schafstall, J., Dengler, M., Brandt, P. and Bange, H. W.: Sea-to-air and diapycnal nitrous oxide fluxes in the eastern tropical North Atlantic Ocean, *Biogeosciences*, 9(3), 957–964, doi:10.5194/bg-9-957-2012, 2012.
- Laruelle, G. G., Cai, W.-J., Hu, X., Gruber, N., Mackenzie, F. T. and Regnier, P.: Continental shelves as a variable but increasing global sink for atmospheric carbon dioxide., *Nat. Commun.*, 9(1), 454, doi:10.1038/s41467-017-02738-z, 2018.
- 785
- Leighton, T. G., Coles, D. G. H., Srokosz, M., White, P. R. and Woolf, D. K.: Asymmetric transfer of CO₂ across a broken sea surface, *Sci. Rep.*, 8(1), 8301, doi:10.1038/s41598-018-25818-6, 2018.
- 790
- M. M. Zweng, Reagan, J. R., Seidov, D., Boyer, T. P., Locarnini, R. A., Garcia, H. E., Mishonov, A. V., Baranova, O. K., Weathers, K., Paver, C. R. and Smolyar, I.: *WORLD OCEAN ATLAS 2018 Volume 2: Salinity* (pre-release).
- 795
- McKenna, S. P. and Bock, E. J.: Physicochemical effects of the marine microlayer on air-sea gas transport, in *Marine Surface Films*, pp. 77–91, Springer-Verlag, Berlin/Heidelberg., 2006.
- Mesarchaki, E., Kräuter, C., Krall, K. E., Bopp, M., Helleis, F., Williams, J. and Jähne, B.: Measuring air–sea gas-exchange velocities in a large-scale annular wind–wave tank, *Ocean Sci.*, 11(1), 121–138, doi:10.5194/os-11-121-2015, 2015.
- 800
- Nightingale, P. D., Malin, G., Law, C. S., Watson, A. J., Liss, P. S., Liddicoat, M. I., Boutin, J. and Upstill-Goddard, R. C.: In situ evaluation of air-sea gas exchange parameterizations using novel conservative and volatile tracers, *Global Biogeochem. Cycles*, 14(1), 373–387, doi:10.1029/1999GB900091, 2000.
- 805
- Pereira, R., Schneider-Zapp, K. and Upstill-Goddard, R. C.: Surfactant control of gas transfer velocity along an offshore coastal transect: results from a laboratory gas exchange tank, *Biogeosciences*, 13(13), 3981–3989, doi:10.5194/bg-13-3981-2016, 2016.
- 810
- Pereira, R., Ashton, I., Sabbaghzadeh, B., Shutler, J. D. and Upstill-Goddard, R. C.: Reduced air–sea CO₂ exchange in the Atlantic Ocean due to biological surfactants, *Nat. Geosci.*, 11(7), 492–496, doi:10.1038/s41561-018-0136-2, 2018.
- 815
- Ravishankara, A. R., Daniel, J. S. and Portmann, R. W.: Nitrous oxide (N₂O): the dominant ozone-depleting substance emitted in the 21st century., *Science*, 326(5949), 123–5, doi:10.1126/science.1176985, 2009.
- 820
- Reynolds, R. W., Smith, T. M., Liu, C., Chelton, D. B., Casey, K. S., Schlax, M. G., Reynolds, R. W., Smith, T. M., Liu, C., Chelton, D. B., Casey, K. S. and Schlax, M. G.: Daily High-Resolution-Blended



- Analyses for Sea Surface Temperature, *J. Clim.*, 20(22), 5473–5496, doi:10.1175/2007JCLI1824.1, 2007.
- 825 Rödenbeck, C., Bakker, D. C. E., Gruber, N., Iida, Y., Jacobson, A. R., Jones, S., Landschützer, P., Metzl, N., Nakaoka, S., Olsen, A., Park, G.-H., Peylin, P., Rodgers, K. B., Sasse, T. P., Schuster, U., Shutler, J. D., Valsala, V., Wanninkhof, R. and Zeng, J.: Data-based estimates of the ocean carbon sink variability - First results of the Surface Ocean pCO₂ Mapping intercomparison (SOCOM), *Biogeosciences*, 12(23), 7251–7278, doi:10.5194/bg-12-7251-2015, 2015.
- 830 Rutgersson, A.: Time series of physical oceanography and carbon dioxide measurements at mooring site OSTERGARNSHOLM - 77FS20150128, PANGAEA, doi:10.1594/PANGAEA.878531, 2017.
- 835 Salter, M. E., Upstill-Goddard, R. C., Nightingale, P. D., Archer, S. D., Blomquist, B., Ho, D. T., Huebert, B., Schlosser, P. and Yang, M.: Impact of an artificial surfactant release on air-sea gas fluxes during Deep Ocean Gas Exchange Experiment II, *J. Geophys. Res.*, 116(C11), C11016, doi:10.1029/2011JC007023, 2011.
- 840 Schuster, U.: Underway physical oceanography and carbon dioxide measurements during Benguela Stream cruise 642B20131005, PANGAEA, doi:10.1594/PANGAEA.852980, 2016.
- 845 Shutler, J. D., Land, P. E., Piolle, J.-F., Woolf, D. K., Goddijn-Murphy, L., Paul, F., Girard-Arduin, F., Chapron, B., Donlon, C. J., Shutler, J. D., Land, P. E., Piolle, J.-F., Woolf, D. K., Goddijn-Murphy, L., Paul, F., Girard-Arduin, F., Chapron, B. and Donlon, C. J.: FluxEngine: A Flexible Processing System for Calculating Atmosphere–Ocean Carbon Dioxide Gas Fluxes and Climatologies, *J. Atmos. Ocean. Technol.*, 33(4), 741–756, doi:10.1175/JTECH-D-14-00204.1, 2016.
- 850 Steinhoff, Tobias; Becker, Meike; Körtzinger, A.: Underway physical oceanography and carbon dioxide measurements during Atlantic Companion cruise 77CN20131004, PANGAEA, doi:10.1594/PANGAEA.852786, 2016.
- 855 Swain, J., Umesh, P. A. and Prasad Kumar, B.: Wave Hindcasting Using WAM and WAVEWATCH III: A Comparison Study Utilizing Oceansat-2 (OSCAT) Winds, *Oceanogr. Mar. Res.*, 5(3), doi:10.4172/2572-3103.1000166, 2017.
- 860 Takahashi, T., Sutherland, S. C., Wanninkhof, R., Sweeney, C., Feely, R. A., Chipman, D. W., Hales, B., Friederich, G., Chavez, F., Sabine, C., Watson, A., Bakker, D. C. E., Schuster, U., Yoshikawa-Inoue, H., Ishii, M., Midorikawa, T., Nojiri, Y., Körtzinger, A., Steinhoff, T., Hoppema, M., Olafsson, J., Arnarson, T. S., Johannessen, T., Olsen, A., Bellerby, R., Wong, C. S., Delille, B., Bates, N. R. and de Baar, H. J. W.: Climatological mean and decadal change in surface ocean pCO₂, and net sea–air CO₂ flux over the global oceans, *Deep Sea Res. Part II Top. Stud. Oceanogr.*, 56(8–10), 554–577, doi:10.1016/J.DSR2.2008.12.009, 2009.
- Villas Boas, A. B., Arduin, F., Ayet, A., Bourassa, M. A., Chapron, B., Brandt, P., Cornuelle, B. D., Farrar, J. T., Fewings, M. R., Fox-Kemper, B., Gille, S. T., Gommenginger, C., Heimbach, P., Hell, M.



- 865 C., Li, Q., Mazloff, M., Merrifield, S. T., Mouche, A., Rio, M., Rodriguez, E., Shutler, J. D., Subramanian, A. C., Terrill, E. J., Tsamados, M., Ubelmann, C. and van Sebille, E.: Integrated observations and modeling of winds, currents, and waves: requirements and challenges for the next decade, *Frontiers in Marine Science* (Accepted), 2019.
- 870 Wanninkhof, Rik; Pierrot, D.: Underway physical oceanography and carbon dioxide measurements during REYKJAFOSS cruise 64RJ20131017, PANGAEA, doi:10.1594/PANGAEA.866092, 2016.
- Wanninkhof, R.: Relationship between wind speed and gas exchange over the ocean, *J. Geophys. Res.*, 97(C5), 7373, doi:10.1029/92JC00188, 1992.
- 875 Wanninkhof, R.: Relationship between wind speed and gas exchange over the ocean revisited, *Limnol. Oceanogr. Methods*, 12(6), 351–362, doi:10.4319/lom.2014.12.351, 2014.
- WAVEWATCH III development group: User manual and system documentation of WAVEWATCH III version 5.16, Technical Note 329., 2016.
- 880 Woolf, D. K., Land, P. E., Shutler, J. D., Goddijn-Murphy, L. M. and Donlon, C. J.: On the calculation of air-sea fluxes of CO₂ in the presence of temperature and salinity gradients, *J. Geophys. Res. Ocean.*, 121(2), 1229–1248, doi:10.1002/2015JC011427, 2016.
- 885 Woolf, D. K., Shutler, J. D., Goddijn-Murphy, L., Watson, A. J., Chapron, B., Nightingale, P. D., Donlon, C. J., Piskozub, J., Yelland, M. J., Ashton, I., Holding, T., Schuster, U., Girard-Ardhuin, F., Grouazel, A., Piolle, A-F., Warren, M., Wrobel-Niedzwiecka, P. E. Land5, R. Torres, J. Prytherch, B. Moat, J. Hanafin, I., Ardhuin, F., and Paul, F.: Key Uncertainties in the Recent Air-Sea Flux of CO₂, *Global Biogeochemical Cycles* (in review), 2019.
- 890 Wrobel, I.: Monthly dynamics of carbon dioxide exchange across the sea surface of the Arctic Ocean in response to changes in gas transfer velocity and partial pressure of CO₂ in 2010, *Oceanologia*, 59(4), 445–459, doi:10.1016/J.OCEANO.2017.05.001, 2017.
- 895 Wrobel, I. and Piskozub, J.: Effect of gas-transfer velocity parameterization choice on air-sea CO₂ fluxes in the North Atlantic Ocean and the European Arctic, *Ocean Sci.*, 12(5), 1091–1091
- 900 Zappa, C. J., McGillis, W. R., Raymond, P. A., Edson, J. B., Hints, E. J., Zemmleink, H. J., Dacey, J. W. H. and Ho, D. T.: Environmental turbulent mixing controls on air-water gas exchange in marine and aquatic systems, *Geophys. Res. Lett.*, 34(10), L10601, doi:10.1029/2006GL028790, 2007.
- 905 Zhao, D., Jia, N. and Dong, Y.: Relationship between turbulent energy dissipation and gas transfer through the air–sea interface, *Tellus B Chem. Phys. Meteorol.*, 70(1), 1–11, doi:10.1080/16000889.2018.1528133, 2018.